4.1.2.3 Sunspots

Sami Solanki, Natalie Krivova

4.1.2.3.1 General characteristics

Sunspots are dark and cool structures on the solar surface harboring a strong magnetic field. They are distinguished from the smaller pores by the fact that they are divided into a darker, usually central umbra and a less dark, peripheral penumbra (Fig. 1). Sunspots are always located within active regions, which, typically, have a bipolar magnetic structure (see Sect. 4.1.2.2.1). The sunspots are thus mainly restricted to the activity belts reaching up to 35° on each side of the solar equator. Their mean latitudes drift from higher to lower latitudes in the course of the sunspot cycle (see Sect. 4.1.2.2.1).

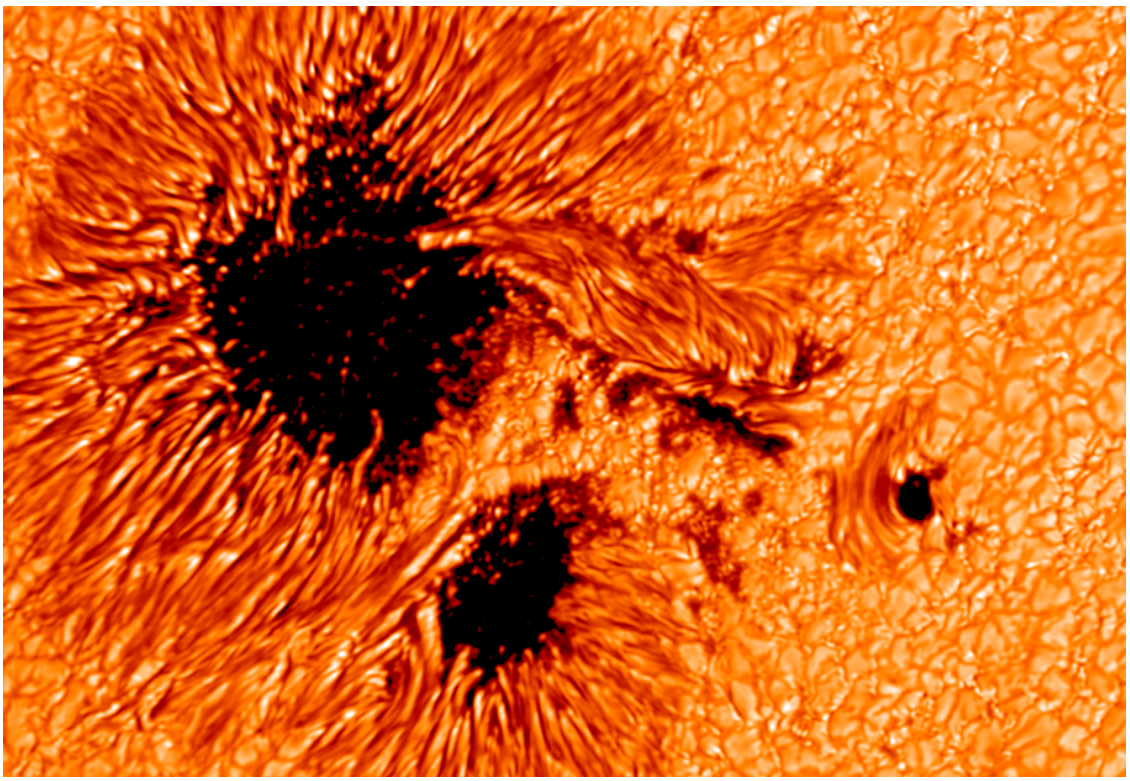

Fig. 1. (see color-picture part, page 616) Image of a complex sunspot with two umbrae observed in the red continuum with the Swedish Solar Telescope on La Palma. With kind permission of J. Hirzberger.

Sunspot sizes range from approximately 3 500 km to 60 000 km (linear dimensions; [b]) and their sizes are lognormally distributed, both if taking a snapshot of sunspots at any given time on the solar surface, or if determining the maximum areas reached by the sunspots in the course of their evolution [88Bog, 05Bau]. The shapes of these size distributions are almost unchanged over the solar activity cycle (but see [04Sol]). The lognormal distribution may be written as:

$$\ln\left(\frac{dN}{dA}\right) = -\frac{(\ln A - \ln\langle A\rangle)^2}{2\ln\sigma_A} + \ln\left(\frac{dN}{dA}\right)_{\max}, \quad (1)$$

where $\langle A\rangle$ is the mean area, σ_A is a measure of the width of the distribution and the last term depends on the size of the sample. Values of the two free parameters of the distribution are given

in Table 1, where we distinguish between a distribution of the (umbral or total) areas of a snapshot of all sunspots at the solar surface, or a distribution of the maximum sizes of sunspots. Results are also given for two different data sets, Mt Wilson (for which umbral areas of individual spots have been analyzed) and Greenwich (which gives both umbral and total spot areas, but only of sunspot groups).

The ratio of total area of sunspot, $r_{\rm tot}$, to umbral area, $r_{\rm u}$, is: $r_{\rm tot}/r_{\rm u} \approx 5 \pm 1$ [d, 90Ste, 91Bra, 93Bec, 05Wen]. This ratio does not depend, or only weakly depends on the size of the sunspot.

Sunspot lifetimes are related to their maximum area by the Gnevyshev-Waldmeier rule: $A_{\rm max} = WT$, where $A_{\rm max}$ is the maximum size of the spot, T its lifetime and $W = 10.89 \pm 0.18$ MSH day^{-1}, where MSH is a Micro Solar Hemisphere, with 1 MSH = $(6.3'')^2$ [97Pet, d].

The decay of sunspot area, dA/dt, is either linear or quadratic; observations give slight support for quadratic decay [97Pet]. For isolated sunspots [93Mar2] give a median $dA/dt = -15$ MSH/day, while for complex sunspot groups $dA/dt = -31$ MSH/day. The decay rate is lognormally distributed [93Mar2, 05Bau], with a tail of very rapidly decaying sunspots. In general, these decay rates are higher than expected from the value of W in the Gnevyshev-Waldmeier rule.

The field strength depends on location within the sunspot. The largest field strength is generally found in the umbra, often nearly co-spatial with the coolest and darkest location [92Kop]. The strongest field strength can cover a large range, with values between 2000 G and over 5000 G having been measured [06Liv]. Values of the maximum field strength below approximately 2 kG are unlikely to be correct, since they are probably affected by straylight [82Bra]. Averaged over the whole sunspot the field strength is roughly 1 kG [93Sol1] and is relatively similar to that in smaller magnetic elements (see Sect. 4.1.2.4.4).

The unit optical depth surface $\tau_{cont} = 1$ is depressed within sunspots compared to the quiet Sun. This is termed the Wilson depression, Z_W. Values differ depending on the method used, lying between 400-800 km for the central umbra [72Gok, 93Mar2, 93Sol2, 04Mat].

Overviews of the properties of sunspots at different levels of detail have been given in various books and review papers [b, c, d, a, f, e, g].

4.1.2.3.2 Intensity and temperature structure

The intensity within a sunspot is highly inhomogeneous. On large scales, within the umbra it can vary by a factor of 2. Intensity profiles of a large and a small sunspot are shown in Fig. 2. The intensity depends strongly on the size or area of a sunspot umbra. At the continuum wavelength $\lambda = 6768$ Å the dependence of the minimum and the average umbral intensity on umbral radius $R_{\rm u}$ is given by a power law [07Mat] while the dependence of the average penumbral intensity is described by a linear function. The coefficients of these functions are given in Table 2.

Table 1. Parameters of lognormal distributions of umbral areas and total sunspot (group) areas [88Bog, 05Bau]. Mt Wilson gives areas of individual umbrae, while Greenwich provides areas of sunspot groups. Max. Dev. means maximum development and signifies that the distribution of the maximum areas reached by the sunspots (sunspot groups) are given. Snapshot means the distribution of areas of all spots present at the solar surface at a given moment in time.

Data set	Method	$\langle A \rangle$	σ_A	No. of spots or groups
Mt. Wilson umbrae	snapshot	0.62	3.80	24 615
Greenwich umbrae	Max. dev.	11.8	2.55	3 966
Greenwich umbrae	Snapshot	12.0	2.24	31 411
Greenwich total area	Max. dev.	62.2	2.45	3 926
Greenwich total area	Snapshot	58.6	2.49	34 562

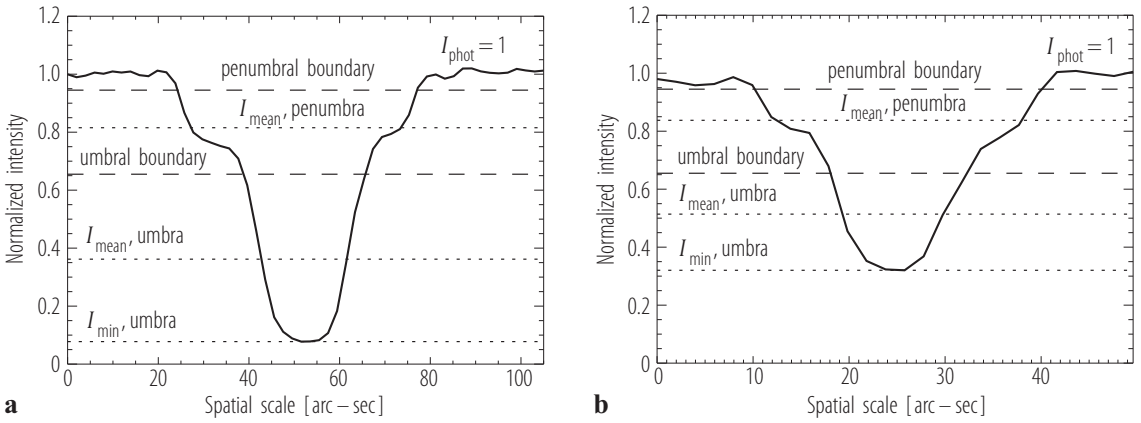

Fig. 2. Cut through two sunspots with different effective umbral radii of around **a)** 15 arcsec and **b)** 6 arcsec. From [07Mat].

The reduced intensity within sunspots can be converted to sunspot umbral effective temperature values. For average umbrae the corresponding temperatures range from 4500 K for umbrae with radii $> 15''$ to 5000 K for umbrae with a radius of $\leq 5''$. Minimum temperatures are lower, reaching as low as 3700 K for the largest umbrae [86Mal]. For the penumbra the effective temperature is typically 5400-5500 K and changes only by $\approx 4\%$ between small and large spots.

It has been proposed that the umbral temperature varies over the solar cycle [78Alb, 84Alb], but different recent investigations have given contradictory results [04Nor, 07Mat, 07Pen]. The only investigation that both uses a homogeneous set of space-based data and properly takes into accout scattered light [07Mat], finds no change of umbral intensity over the solar cycle.

The intensity contrast of the sunspot umbra and penumbra depends on the wavelength. Values published for the minimum intensity in the umbrae of very large sunspots are given in Table 3 [78Alb, 84Alb, 72Mal, 86Mal], cf. [c]. They agree with the minimum intensity of the largest umbrae observed with MDI [07Mat]. Given are the intensity contrasts, $i_u(\mu = 1, \lambda) = I_u/I_{QS}$, where I_u is the minimum intensity in the umbra and I_{QS} is the average quiet Sun intensity, $i_p(\mu = 1, \lambda) = I_p/I_{QS}$, where I_p is the average penumbral intensity, and the linear limb darkening coefficient for the umbral contrast b_u, which enters the relationship for the centre-to-limb variation of umbral contrast:

$$i_u(\mu, \lambda) = i_u(\mu = 1, \lambda) - b_u(1 - \mu). \quad (2)$$

Here $\mu = \cos\theta$ and θ is the angle betwen the line of sight and the surface normal.

The presence of a sunspot on the solar disc leads to a reduction of the Sun's irradiance [81Wil]. To describe the Sun's darkening due to passages of N sunspots across the solar disc, the photometric

Table 2. Constant and exponent of power law fits to umbral core (minimum) and mean intensity as a function of umbral radius. Also, the constant and gradient of a linear fit to penumbral mean intensity vs. umbral radius. These relations were derived from data from which the scattered light has been removed [07Mat].

Dependence on umbral radius of,	umbral radius	Constant	Exponent	Gradient
umbral core intensity	all	1.8598	−1.0679	
umbral mean intensity	all	0.8297	−0.3052	
penumbral mean intensity	$> 10''$	0.8561		−0.0016

sunspot index, PSI, is used [82Hud, 94Fro]:

$$PSI = \frac{\sum_{i=1,N} \Delta S_i}{S_{\rm QS}}, \tag{3}$$

where ΔS_i is the reduction in solar brightness caused by each individual sunspot relative to the quiet Sun, $S_{\rm QS}$, and the summation is done over all sunspots present on the solar visible surface at the time of observation. If $A_{\rm s}$ is the spot area in fractions of the solar hemisphere (see Sect. 4.1.2.2.1), $i_{\rm s} = I_{\rm s}/I_{\rm QS}$ is the spot contrast and $f(\mu)$ is the centre-to-limb variation of the brightness and of the spot (here an assumption is usually made that the limb darkening law is the same for the quiet Sun and spots), then the following equation for the PSI is obtained:

$$PSI = \sum \mu A_{\rm s} \, (i_{\rm s} - 1) \, \frac{f(\mu)}{\int_0^1 \mu f(\mu) {\rm d}\mu}. \tag{4}$$

Based on observations of 130 spots and spot groups, the following empirical relationship for $1 - i_{\rm s}$ is deduced [94Bra], which takes into account its dependence on the spot area:

$$\alpha = 1 - i_{\rm s} = 0.2231 + 0.0244 \cdot \log(A_{\rm s}). \tag{5}$$

A part, $< 10\%$ of the blocked energy reappears in a bright ring around a sunspot [99Ras, 01Ras].

Recent models of the core (coolest part) of the umbra of a large sunspot (umbral radius $> 15''$, model S; Table 4) and the penumbra (model R; Table 5) have been given by [06Fon]. Although the authors call it a model of an average umbra of an average sunspot, it appears to describe a rather cool umbra. For smaller umbrae, as well as for most positions within an umbra hotter models are required. Earlier umbral models are due to [84Van, 86Mal, 88Obr]. Of particular interest is the model of [93Cac], who found that in order to reproduce the wings of strong lines in the visible the photospheric temperature gradient must be steep.

4.1.2.3.3 Magnetic field structure

The magnetic field strength of a regular sunspot (i.e. a sunspot with a single umbra surrounded by an intact penumbra) drops steadily from the centre of the spot towards its edge and becomes increasingly horizontal. The maximum field strength of a spot varies with size of the spot, as given in Table 6. The largest measured field strength in a sunspot is 6100 G [06Liv]. The fraction of spots with a given maximum field strength decreases steadily with increasing maximum field strength. The percentages of groups with strongest fields > 3 kG is 4.6%; > 3.5 kG is 1.5%; > 4 kG is 0.4% and > 4.5 kG is 0.09% [06Liv].

The field strength and inclination angle of the field to the vertical are tabulated vs. the distance to the sunspot's centre, normalized to the radius of the sunspot for a large, regular sunspot, by [c]. For a sufficiently regular sunspot the projection of the field on the solar surface (i.e. the horizontal component of the field) points in a radial direction within about 20°, i.e. sunspots display little twist. The field in the penumbra shows, on average, a significant inclination towards the horizontal, so that considerable magnetic flux must appear through the penumbra (i.e. the penumbra must be deep). Estimates of the amount of magnetic flux appearing in the umbra, $\Phi_{\rm u}$, relative to the

Table 3. Maximum intensity contrast in umbra relative to quiet Sun, $i_{\rm u}$, and mean penumbral intensity contrast, $i_{\rm p}$, at disc centre ($\mu = 1$), as well as the centre-to-limb coefficient, $b_{\rm u}$, of the umbral contrast.

λ [μm]	0.387	0.579	0.669	0.876	1.215	1.54	1.67	1.73	2.09	2.35	3.8
$i_{\rm u}(\mu = 1, \lambda)$	0.008	0.066	0.090	0.215	0.345	0.495	0.548	0.577	0.589	0.581	
$b_{\rm u}(\lambda)$	–0.010	0.012	0.009	0.019	0.031	0.087	0.087	0.094	0.090	0.058	
$i_{\rm p}(\mu = 1, \lambda)$	0.64	0.768	0.794	0.827	0.876		0.914		0.928		0.936

Table 4. Umbral model atmosphere (model S [06Fon]).

Height [km]	Temperature [K]	Gas pressure [dyne cm^{-2}]
4.278E+02	3.593E+03	2.285E+03
3.501E+02	3.587E+03	5.590E+03
2.698E+02	3.600E+03	1.399E+04
1.978E+02	3.611E+03	3.160E+04
1.333E+02	3.642E+03	6.480E+04
8.099E+01	3.692E+03	1.151E+05
4.330E+01	3.772E+03	1.719E+05
1.798E+01	3.896E+03	2.226E+05
6.451E-01	4.040E+03	2.652E+05
–9.587E+00	4.170E+03	2.921E+05
–1.968E+01	4.320E+03	3.208E+05
–2.958E+01	4.490E+03	3.513E+05
–3.871E+01	4.680E+03	3.799E+05
–4.796E+01	4.890E+03	4.096E+05
–5.826E+01	5.120E+03	4.442E+05
–6.888E+01	5.360E+03	4.801E+05
–8.143E+01	5.620E+03	5.255E+05
–9.311E+01	5.870E+03	5.685E+05
–1.072E+02	6.140E+03	6.222E+05
–1.184E+02	6.420E+03	6.689E+05
–1.284E+02	6.700E+03	7.122E+05
–1.385E+02	7.000E+03	7.564E+05

Table 5. Penumbral model atmosphere (model R [06Fon]).

Height [km]	Temperature [K]	Gas pressure [dyne cm^{-2}]
4.198E+02	4.590E+03	4.120E+03
3.917E+02	4.622E+03	5.327E+03
3.637E+02	4.658E+03	6.875E+03
3.357E+02	4.701E+03	8.853E+03
3.075E+02	4.727E+03	1.138E+04
2.794E+02	4.759E+03	1.462E+04
2.511E+02	4.801E+03	1.876E+04
2.226E+02	4.856E+03	2.404E+04
1.937E+02	4.927E+03	3.080E+04
1.826E+02	4.951E+03	3.382E+04
1.674E+02	4.972E+03	3.843E+04
1.519E+02	4.991E+03	4.373E+04
1.361E+02	5.044E+03	4.986E+04
1.197E+02	5.115E+03	5.696E+04
1.028E+02	5.218E+03	6.523E+04
8.504E+01	5.356E+03	7.489E+04
6.635E+01	5.517E+03	8.621E+04
5.056E+01	5.637E+03	9.675E+04
4.160E+01	5.740E+03	1.031E+05
3.125E+01	5.826E+03	1.109E+05
2.163E+01	5.939E+03	1.185E+05
1.099E+01	6.101E+03	1.272E+05
–3.555E-01	6.290E+03	1.369E+05
–1.201E+01	6.452E+03	1.473E+05
–2.362E+01	6.630E+03	1.580E+05
–3.508E+01	6.809E+03	1.690E+05
–4.622E+01	7.015E+03	1.801E+05
–5.707E+01	7.223E+03	1.912E+05
–6.763E+01	7.443E+03	2.023E+05
–7.795E+01	7.682E+03	2.133E+05
–8.814E+01	7.980E+03	2.244E+05
–9.829E+01	8.215E+03	2.355E+05
–1.165E+02	8.616E+03	2.560E+05
–1.269E+02	8.845E+03	2.677E+05

total magnetic flux of the sunspot, $\Phi_{\rm tot}$, and of the magnetic flux appearing in the penumbra, $\Phi_{\rm p}$, relative to $\Phi_{\rm tot}$ are [93Sol1]:

$$\Phi_{\rm u}/\Phi_{\rm tot} = 1/3 \div 1/2, \qquad \Phi_{\rm p}/\Phi_{\rm tot} = 1/2 \div 2/3. \tag{6}$$

In the umbra, the field strength is related to intensity or, equivalently, temperature. Within the umbra the squared field strength B^2 increases nearly *linearly* with decreasing temperature [93Mar1, 93Sol2, 94Bal, 04Mat]. Consequently, also the maximum field strength of the sunspot depends on its minimum temperature [92Kop, 02Liv]. Across the umbral boundary this relationship changes and becomes strongly non-linear.

Within the visible outline of the sunspot the field strength decreases with height. In the umbra, at photospheric levels $|\partial B/\partial z| \approx$ 1–3 G km^{-1} [93Bal, 95Bru, 00Eib]. When averaged over a height range of 2000 km or more $|\partial B/\partial z|$ is reduced to 0.3-0.6 G km^{-1} [82Hen, 93Lee, 95Pen].

The gradient of the field depends on the field strength [95Pen] and hence on the position in the sunspot (the larger the field the larger the gradient, so that the field is more homogeneous in the chromosphere than in the photosphere).

At the outer edge of the sunspot the magnetic field has a strength of 700-1000 G and is inclined by $70 - 80°$ relative to the surface normal. The field does not stop there (at photospheric layers). A part of it returns into the solar interior there [97Wes]. Another part continues in the form of a magnetic canopy, i.e. a nearly horizontal magnetic field overlying comparatively field-free gas. Canopies have been followed up to a distance of roughly 2 sunspot radii from the centre of a sunspot. Their base heights increase very slowly with distance from the spot. At a distance of 2 spot radii the canopy still lies only 300-350 km above the quiet-Sun $\tau_{500} = 1$ [80Gio, 82Gio, 99Sol].

4.1.2.3.4 Flows and oscillations

Photospheric spectral lines display a blueshift on the discward side of the penumbra and a redshift on the limbward side. This pattern of line shifts is termed the Evershed effect. In the chromosphere the opposite behaviour is observed, the inverse Evershed effect e.g., [09Eve, 13StJ, 61Hol, 88Ali, 00Sch, 02Rou, d]. The Evershed effect is interpreted as a nearly horizontal outflow of material. Typical velocities associated with the photospheric Evershed effect are small in the inner penumbra and steadily increase to 1-2 km s^{-1} in the outer penumbra, when measured at low to intermediate spatial resolution. At high resolution (and from spectral inversions) the Evershed flow is found to be restricted to the horizontal magnetic field component, where it typically shows maximum speed of 3-4 km s^{-1} and can display speeds as high as 6-9 km s^{-1} depending on the spectral line [03Pen]. The Evershed flow becomes supersonic at some places in the penumbra [05Bor, 08Bel]. In the inner penumbra, material is seen to rise [00Sch] while in the outer penumbra a significant fraction of the outflowing material returns into the solar interior [97Wes], so that only roughly 10% of the gas continues to flow out above the base of the magnetic canopy outside the sunspot [94Sol].

Typically, the strength of the Evershed effect decreases as one consideres lines formed higher in the atmosphere. Above the temperature minimum the flow displays an inward motion. The inverse Evershed flow is seen throughout the chromosphere and up into the transition region. Upflow velocities of 1-6 km s^{-1} are derived from H-alpha [03Geo]. The inverse Evershed flow is nearly horizontal outside the sunspot and increasingly more vertical closer to the umbra. Above the umbra strongly temperature-dependent downflows are observed, ranging from 5 km s^{-1} seen in chromospheric lines (e.g., of O I 1355.50 Å) to approximately 40 km s^{-1} in O V 1371.29 Å. At higher temperature the flow velocity decreases again and no downflow is observed in coronal lines, such as Fe XII 1349.40 Å [99Bry].

4.1.2.3.5 Sunspot fine structure

Both umbrae and penumbrae show significant fine structure in intensity images and in the magnetic field. In umbrae the main fine structure features are umbral dots, while in penumbrae they are penumbral filaments (with dark lanes) and bright grains (see Fig. 1).

Umbral dots: umbral dots have a distribution of sizes ranging from 100 km (the resolution limit of current observations) to 300-400 km, with the most common size being around 200 km.

Table 6. Maximum magnetic field strength B_{max} as a function of umbral radius. From [c], cf. [82Bra, 92Kop].

Umbral radius [km]	1000	2000	4000	6000	8000	1000
B_{max} [G]	2000	2000	2300	2700	3100	3500

Similarly, they have a range of brightnesses covering 0.2–1.2I_{QS} in the visible and a contrast of on average 1.8 relative to the umbral background at a wavelength of 450 nm [05Sob]. At 700 nm this contrast drops to roughly 1.2 (but depends in detail on the intensity of the umbral background; [08Rie2]). In their centres umbral dots display a narrow dark lane [06Sch, 07Bha].

Umbral dots display a weaker field (by about 500 G) than the surrounding umbral background, with the reduction being limited to the lowest observable layers [04Soc, 08Rie1]. These layers also reveal an upflow up to 800 m s^{-1}. The observations are consistent with MHD simulations [06Sch], according to which umbral dots are convective upwellings.

One distinguishes between central umbral dots, found in the inner part of the umbra (less bright, nearly stationary) and peripheral umbral dots (brighter, on average moving away from the penumbra). The latter often result when penumbral grains enter the umbra [86Gro, 08Rie1].

Penumbral fine structure: The penumbra is dominated by bright filaments separated by a dark background. These filaments have a length of 0.5–2″, but can also be longer, and a width of 0.2-0.6″. They live for 10 min to 4 hours [d, 73Mul, 82Ton, 95Den, 99Sob, 02Sch, 03Sol]. They have a distribution of brightness $\approx 0.6-0.8 I_{QS}$ for the dark component and $\approx 0.8-1.1 I_{QS}$ for the bright [73Mul, 81Gro, 88Col]. At the inner ends of bright penumbral filaments are bright dot-like structures called penumbral grains that move towards the umbra at a speed of roughly 0.4 km s^{-1} [99Sob]. At the highest resolution bright penumbral filaments display a dark lane down their middle [02Sch]. When observed at a heliocentric angle of 30-50° the filaments display a twisting motion [07Ich], which has been interpreted as a manifestation of magnetoconvection similar to convective rolls [08Zak, 61Dan].

A large fraction of sunspots contain light bridges, which separate an umbra into two parts, or separate two umbrae (if the light bridge is sufficiently broad and bright). Light bridges can have brightnesses ranging from less than that of the penumbra up to that of the photosphere. Light bridges display a reduction in field strength of 200-1500 G relative to the umbra [97Lek]. The field is also more horizontal by $5-30°$ [69Bec, 91Lit, 95Rue].

Moving magnetic features are found in the moat outside the sunspot. As the name suggests, they travel away from the spot. Three types of moving magnetic features are distinguished [01Shi].

Type I: they are composed of a pair of opposite polarity magnetic features, with the feature closer to the spot having opposite polarity to the spot [03Zha]. They move away from spot at a speed of 0.5-1 km s^{-1}. They are best explained in terms of U-shaped loops.

Type II: these are single magnetic features having the same polarity as the sunspot. They travel at a speed of 0.5-1 km s^{-1}.

Type III: these single magnetic features have a magnetic polarity opposite to the sunspot. They travel away from spot at a speed of 2-3 km s^{-1}.

4.1.2.3.6 References for 4.1.2.3

General references

a Bellot Rubio, L.R.: Rev. Mod. Astr. **17** (2004) 21.

b Bray, R.J., Loughhead, R.E.: Sunspots, The International Astrophysics Series, London: Chapman & Hall (1964).

c Solanki, S.K.: Sunspots, in Allen's Astrophysical Quantities, (A.N. Cox, W.C. Livingston, Eds.), New York: Springer-Verlag (1999) 367.

d Solanki, S.K., Astron. Astrophys. Rev. **11** (2003) 153

e Solanki, S.K., Inhester, B., Schüssler, M.: Rep. Prog. Phys. **69** (2006) 563.

f Thomas and Weiss: Ann. Rev. Astron. Astrophys. **42** (20004) 517.

g Weiss, N.O.: Space Sci. Rev. **124** (2006) 13.

Special references

13StJ St. John, Ch.E.: Astrophys. J. **37** (1913) 322.
61Dan Danielson, R.E.: Astrophys. J. **134** (1961) 289.
61Hol Holmes, J.: MNRAS **122** (1961) 301.
69Bec Beckers, J.M., Schröter, E.H.: Solar Phys. **10** (1969) 384.
72Gok Gokhale, M.H., Zwaan, C.: Sol. Phys. **26** (1972) 52.
72Mal Maltby, P.: Sol. Phys. **26** (1972) 76.
73Mul Muller, R.: Sol. Phys. **29** (1973) 55 (in french).
78Alb Albregtsen, F., Maltby, P.: Nature **274** (1978) 41.
80Gio Giovanelli, R.G.: Sol. Phys. **68** (1980) 49.
81Gro Grossmann-Doerth, U., Schmidt, W.: Astron. Astrophys. **95** (1981) 366.
81Wil Willson, R.C., Gulkis, S., Janssen, M., Hudson, H.S., Chapman, G.A.: Science **211** (1981) 700.
82Bra Brants, J.J., Zwaan, C.: Sol. Phys. **80** (1982) 251.
82Gio Giovanelli, R.G., Jones, H.P.: Sol. Phys. **79** (1982), 267.
82Hen Henze, W., Tandberg-Hanssen, E., Hagyard, M.J., West, E.A., Woodgate, B.E., Shine, R.A., Beckers, J.M., Bruner, M., Hyder, C.L., West, E.A.: Sol. Phys.**81** (1982) 231.
82Hud Hudson, H.S., Silva, S., Woodard, M., Willson, R.C.: Solar Phys. **76** (1982) 211.
82Ton Tönjes, K., Wöhl, H.: Sol. Phys. **75** (1982) 63.
84Alb Albregtsen, F., Jorås, P.B., Maltby, P.: Sol. Phys. **90** (1984) 17.
84Van Van Ballegooijen, A.A.: Solar Phys. **91** (1984) 195.
86Gro Grossmann-Doerth, U., Schmidt, W., Schroeter, E.H.: Astron. Astrophys. **156** (1986) 347.
86Mal Maltby, P., Avrett, E.H., Carlsson, M., Kjeldseth-Moe, O., Kurucz, R.L., Loeser, R.: Ap. J. **306** (1986) 284.
88Ali Alissandrakis, C.E., Dialetis, D., Mein, P., Schmieder, B., Simon, G.: Astron. Astrophys. **201** (1988) 339.
88Bog Bogdan, T.J., Gilman, P.A., Lerche, I., Howard, R.: Astrophys. J. **327** (1988) 451.
88Col Collados, M., del Toro Iniesta, J.C., Vazquez, M.: Astron. Astrophys. **195** (1988) 315.
88Obr Obridko, V.N., Staude, J.: Astron. Astrophys. **189** (1988) 232.
90Ste Steinegger, M., Brandt, P.N., Pap, J., Schmidt, W.: Astrophys. Space Sci. 170 (1990) 127.
91Lit Lites, B.W., Bida, T.A., Johannesson, A., Scharmer, G.B.: Astrophys. J. **373** (1991) 683.
91Bra Brandt, P.N., Schmidt, W., Steinegger, M.: Sol. Phys. **129** (1991) 191.
92Kop Kopp, G., Rabin, D.: Solar Phys. **141** (1992) 253.
93Bal Balthasar, H., Schmidt, W.: Astron. Astrophys. **279** (1993) 243.
93Bec Beck, J.G., Chapman, G.A.: Sol. Phys. **146** (1993) 49.
93Cac Caccin, B., Gomez, M.T., Severino, G.: Astron. Astrophys. **276** (1993) 219.
93Lee Lee, J.W., Hurford, G.J., Gary, D.E.: Sol. Phys. **144** (1993) 45.
93Mar1 Martínez Pillet, V., Vázquez, M.: Astron. Astrophys. **270** (1993) 494.
93Mar2 Martínez Pillet, V., Moreno-Insertis, F., Vázquez, M.: Astron. Astrophys. **274** (1993) 521.
93Sol1 Solanki, S.K., Schmidt, H.U.: Astron. Astrophys. **267** (1993) 287.
93Sol2 Solanki, S.K., Walther, U., Livingston, W.: Astron. Astrophys. **277** (1993) 639.
94Bal Balthasar, H., Schmidt, W.: Astron. Astrophys. **290** (1994) 649.
94Bra Brandt, P.N., Stix, M., Weinhardt, H.: Sol. Phys. **152** (1994) 119.
94Fro Fröhlich, C., Pap, J.M., Hudson, H.S.: Solar Phys. **152** (1994) 111.
94Sol Solanki, S.K., Montavon, C.A.P., Livingston, W.: Astron. Astrophys. **283** (1994) 221.
95Bru Bruls, J.H.M.J., Solanki, S.K., Rutten, R.J., Carlsson, M.: Astron. Astrophys. **293** (1995) 225.

95Den Denker, C., de Boer, C.R., Volkmer, R., Kneer, F.: Astron. Astrophys. **296** (1995) 567.
95Pen Penn, M.J., Kuhn, J.R.: Astrophys. J. Lett. **441** (1995) L51.
95Rue Rüedi, I., Solanki, S.K., Livingston, W.: Astron. Astrophys. **302** (1995) 543.
97Lek Leka, K.D.: Astrophys. J. **484** (1997) 900.
97Pet Petrovay, K., van Driel-Gesztelyi, L.: Solar Phys. **176** (1997) 249.
97Wes Westendorp Plaza, C., del Toro Iniesta, J.C., Ruiz Cobo, B., Martínez Pillet, V., Lites, B.W., Skumanich, A.: Nature **389** (1997) 47.
99Bry Brynildsen, N., Maltby, P., Brekke, P., Haugan, S.V.H., Kjeldseth-Moe, O.: Sol. Phys. **186** (1999) 141.
99Ras Rast, M.P., Fox, P.A., Lin, H., Lites, B.W., Meisner, R.W., White, O.R.: Nature **401** (1999) 678.
99Sob Sobotka, M., Brandt, P.N., Simon, G.W.: Astron. Astrophys. **348** (1999) 621.
99Sol Solanki, S.K., Finsterle, W., Rüedi, I., Livingston, W.: Astron. Astrophys. **347** (1999), L27.
00Eib Eibe, M.T., Aulanier, G., Faurobert, M., Mein, P., Malherbe, J.M.: Astron. Astrophys. **381** (2000) 290.
00Sch Schlichenmaier, R., Schmidt, W.: Astron. Astrophys. **358** (2000) 1122.
01Ras Rast, M.P., Meisner, R.W., Lites, B.W., Fox, P.A., White, O.R.: Astrophys. J. **557** (2001) 864.
01Shi Shine, R.A., Title, A.M.: in Encyclopedia of Astron. Astrophys., Bristol: Inst. of Phys. Publishing **4** (2001) 3209.
02Liv Livingston, W.: Sol. Phys. **207** (2002) 41.
02Rou Rouppe van der Voort, L.H.M.: Astron. Astrophys. **389** (2002) 1020.
02Sch Scharmer, G.B., Gudiksen, B.V., Kiselman, D., Löfdahl, M.G., Rouppe van derVoort, L.H.M.: Nature **420** (2002) 151.
03Geo Georgakilas, A.A., Christopoulou, E.B., Skodras, A., Koutchmy, S.: Astron. Astrophys. **403** (2003) 1123.
03Pen Penn, M.J., Cao, W.D., Walton, S.R., Chapman, G.A., Livingston, W.: Atrophys. J. Lett. **590** (2003) L119.
03Sol Solanki, S.K., Rüedi, I.: Astron. Astrophys. **411** (2003) 249.
03Zha Zhang, J., Solanki, S.K., Wang, J.: Astron. Astrophys. **399** (2003) 755.
04Mat Mathew, S.K., Solanki, S.K., Lagg, A., Collados, M., Borrero, J.M., Berdyugina, S.: Astron. Astrophys. **422** (2004) 693.
04Nor Norton, A.A., Gilman, P.A.: Astrophys. J. **603** (2004) 348.
04Soc Socas-Navarro, H., Martínez Pillet, V., Sobotka, M., Vázquez, M.: Astrophys. J. **614** (2004) 448.
04Sol Solanki, S.K., Unruh, Y.C.: Mon. Not. Royal Astron. Soc. **348** (2004) 307.
05Bau Baumann, I., Solanki, S.K.: Astron. Astrophys. **443** (2005) 1061.
05Bor Borrero, J.M., Lagg, A., Solanki, S.K., Collados, M.: Astron. Astrophys. **436** (2005) 333.
05Sob Sobotka, M., Hanslmeier, A.: Astron. Astrophys. **442** (2005) 323.
05Wen Wenzler, T.: Reconstruction of Solar Irradiance Variations in Cycles 21-23 based on Surface Magnetic Fields, PhD Thesis, ETH Zürich (2005).
06Fon Fontenla, J.M., Avrett, E., Thuillier, G., Harder, J.: Astrophys. J. **639** (2006) 441.
06Liv Livingston, W.C., Harvey, J.W., Malanushenko, O.V., Webster, L.: Sol. Phys. **239** (2006) 41.
06Sch Schüssler, M., Vögler, A.: Astrophys. J. **641** (2006) L73.
07Bha Bharti, L., Jain, R., Jaaffrey, S.N.A.: Astrophys. J. **665** (2007) L79.
07Ich Ichimoto, K., Suematsu, Y., Tsuneta, S., Katsukawa, Y., Shimizu, T., Shine, R.A., Tarbell, T.D., Title, A.M., Lites, B.W., Kubo, M., Nagata, S.: Science **318** (2007) 1597.

07Mat Mathew, S.K., Martínez Pillet, V., Solanki, S.K., Krivova, N.A.: Astron. Astrophys. **465** (2007) 291.
07Pen Penn, M.J., MacDonald, R.K.D.: Astrophys. J. Lett. **662** (2007) L123.
08Bel Bellot Rubio, L.R., Tritschler, A., Martínez Pillet, V.: Astrophys. J. **676** (2008) 698.
08Rie1 Riethmüller, T., Solanki, S.K., Lagg, A.: Astrophys. J. Lett. **678** (2008) L157.
08Rie2 Riethmüller, T., Solanki, S.K., Zakharov, V., Gandorfer, A.: Astron. Astrophys. **492** (2008) 233.
08Zak Zakharov, V., Hirzberger, J., Riethmüller, T.L., Solanki, S.K., Kobel, P.: Astron. Astrophys. **488** (2008) L17.
09Eve Evershed, J.: MNRAS **69** (1909) 454.